PERGAMON

Vacuum 62 (2001) 263–271

VACUUM
SURFACE ENGINEERING, SURFACE INSTRUMENTATION & VACUUM TECHNOLOGY

www.elsevier.nl/locate/vacuum

Electron beam lithography simulation for high resolution and high-density patterns

I. Raptis[a,b,*], N. Glezos[a], E. Valamontes[b], E. Zervas[b], P. Argitis[a]

[a]*Institute of Microelectronics, NCSR "DEMOKRITOS", 15310 Ag.Paraskevi Attikis, Greece*
[b]*Electronics Department, Technological Institute of Athens, Ag. Spiridonos 12 12243 Aegaleo, Greece*

Received 27 June 2000; accepted 10 November 2000

Abstract

A fast simulator for electron beam lithography, called SELID™, is applied for the simulation and prediction of the resist profile of high-resolution patterns in the case of homogeneous and multilayer substrates. For exposure simulation, an analytical solution based on the Boltzmann transport equation (where all important scattering phenomena have been taken into account) for a wide range of e-beam energies is used. The case of substrates consisting of more than one layer (multilayer) is considered in depth as it is of great importance in e-beam patterning. By combining the energy deposition data from simulation with analytical functions describing the resist development (for the conventional positive-resist PMMA), complete simulation of dense layouts in the sub-quarter-micron range has been carried out. Additionally, the simulation results are compared with experimental ones for dense patterns in the sub-quarter-micron region. By using SELID™, forecast of resist profile with considerable accuracy for a wide range of resists, substrates and energies is possible, reducing in that way the cost of process development. Additionally, proximity effect parameters are extracted easily for use in any proximity correction package. © 2001 Elsevier Science Ltd. All rights reserved.

Keywords: Electron beam lithography; Boltzmann transport equation; Proximity effect; Nanofabrication

1. Introduction

During the last decades electron beam lithography has been used intensively for the development of prototype devices and for the exploration of future devices (nanotechnology). Additionally, since the device critical dimensions for high-performance integrated circuits (ICs) nowadays are in the sub-0.25 μm range, electron beam lithography plays an important role also in mask making processes for these ICs. In the future, the use of electron beam lithography is expected to increase through the application of e-beam lithography tools in mass production in mix and match lithography schemes [1] (direct write using raster, shaped and projection e-beam lithography tools e.g. PREVAIL [2], SCALPEL [3]) and in nanotechnology. Therefore, the understanding of electron beam interactions with matter and the physicochemical changes associated with these interactions are of vital importance for the optimization of the whole lithographic process.

* Correspondence address. Institute of Microelectronics, NCSR "DEMOKRITOS", 15310 Ag. Paraskevi Attikis, Greece. Fax: + 3-01-6511723.

E-mail address: raptis@imel.demokritos.gr (I. Raptis).

0042-207X/01/$ - see front matter © 2001 Elsevier Science Ltd. All rights reserved.
PII: S0042-207X(00)00448-6

Lithography modeling has been proven an adaptable tool in the efforts for the improvement of optical and e-beam lithography over the last years. However, since the resolution required in mask making was not so challenging in the past, the main target of electron beam lithography simulation tools was the correction of the so-called proximity effect.

In the current work, simulation results for thin resist layers on homogeneous and multilayer substrates for a wide range of e-beam energies using a novel electron beam lithography simulator are presented (SELID™ [4] commercialized by SIGMA-C, Germany). The simulation results obtained from this simulation tool are compared with experiment. The comparison is carried out for high-resolution conditions e.g. high e-beam energy (50 keV), thin resist films (0.4–0.8 μm) and appropriate resist for high-resolution (conventional positive tone, PMMA). It is shown that, SELID™ is capable of simulation of dense patterns with critical dimension in the sub-quarter-micron range.

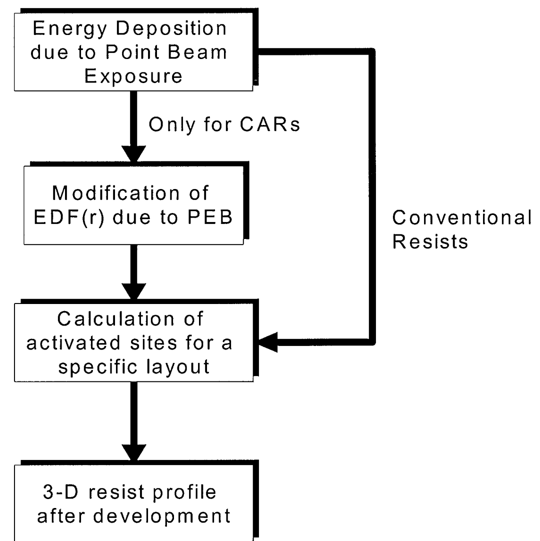

Fig. 1. SELID simulation flow chart. In the case of chemically amplified resists, an additional step for the evaluation of acid concentration is required. In all cases, results from previous simulation runs can be used in order to decrease the required CPU time.

2. Structure of the simulation tool

This simulation tool is structured in three modules (Fig. 1). In the first module the energy deposition EDF(r) in the resist film due to a "point" beam electron source is calculated using an analytical model based on a solution of the Boltzmann transport equation[1] [5–7]. EDF(r) is the fundamental quantity for e-beam lithography simulation since it is independent of the layout to be exposed, the beam properties (viz. shape, dimensions) and exposure strategy (raster or vector). Thus, the energy deposition of the first module can be used in all simulation cases where the beam energy and the composition of the resist and substrate films (in terms of materials and thickness) are the same.

The second module actually consists of two parts. In the first, the beam shape and dimensions are taken into account (single pixel exposure, SEDF(r)) through appropriate convolution of the energy deposition calculated in first module. In the second part the SEDF(r) is convolved with the actual layout to be simulated. This part and consequently the second module is the most CPU time consuming of the whole simulation procedure, since the energy deposition to a specific point in a considered layout depends strongly on the layout mainly through the contribution of backscattered electrons. The influence range of the backscattered electrons depends strongly on the composition of the substrate and the beam energy. Therefore, the CPU time required also depends on these parameters. The influence range used in simulations must be selected carefully in order to keep the CPU time required small without degradation of simulation accuracy (e.g. for 10 keV exposure on bulk PMMA on bulk Si substrate the influence range must be at least 1 μm while, in the 50 keV case, at least 10 μm).

The final energy deposition is used as input for the simulation of resist development (third module). In this module, a complete set of development models is available in the software for selection. By

[1] Recently, the application of the Boltzmann transport equation has been extended to low e-beam energies with promising results [8].

applying the development rate of the specific resist, the final resist profile in two and three dimensions is calculated for the assumed development conditions.

In the case of chemically amplified resists the processing requires one more step after the exposure: the post exposure bake (PEB), where the chemical changes in the resist film take place. In SELID™ the simulation of this step takes place on the EDF(r) even though the PEB step happens after exposure. This simulation strategy offers the advantage of small CPU times when various layouts are under investigation. If the PEB simulation is done on the final layout then a huge amount of CPU time is required, since simulation has to take place on a much larger matrix (3-D).

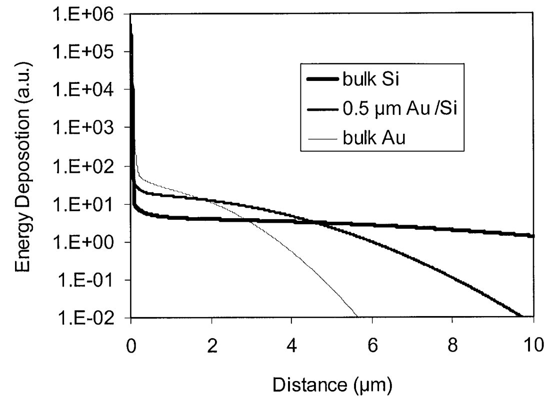

Fig. 2. EDF(r) at the resist/substrate interface for various substrates (homogeneous, multi layer).

3. Energy deposition calculations

The method applied for the calculation of EDF(r) is based on the Boltzmann transport equation and it is well documented in the literature [5–8]. This method has been developed for the simulation of energy deposition in thin resist films on homogeneous substrates (i.e. bulk Si) and extended for substrates consisting of horizontal layers of different materials (multilayer). The second case is most usual in IC fabrication since every device consists of several layers of different materials (i.e. Si, Si_3N_4, SiO_2, Al, etc.). Additionally, the mask plate consists of two layers: 0.1 μm Cr on glass. As shown in Fig. 2, the substrate cross-section affects significantly the energy deposition, so that the substrate composition must be taken into account in a detailed manner.

Since EDF(r) is calculated using analytical functions the required CPU time is very small allowing the use of a very fine grid. In Table 1 the CPU times required for various grid values and e-beam energies are listed. For the simulation a Pentium III — 500 MHz (256 MB memory) was used. From this table it is obvious that the CPU time in all cases is very small and varies linearly with the range in the X-axis (axis vertical to the axis of incidence Z-axis). It must be noted that the CPU time does not depend on the substrate composition (homogeneous or multilayer); this is not the case for the Monte Carlo method [9–11] where the existence of an interface implies additional conditional statements in the code.

Table 1
CPU times required for various substrate composition and e-beam energies

Resist/substrate	Energy (keV)	D_z (nm)	D_x (nm)	X-range (pixels)	CPU time (s)
0.4 μm PMMA/Si	50	20	10	2000	20
0.4 μm PMMA/Si	50	20	5	4000	40
0.4 μm PMMA/Si	10	20	10	400	9
0.4 μm PMMA/Si	10	20	5	800	18
0.4 μm PMMA/Si	50	10	10	2000	55
0.4 μm PMMA/0.5 μm Au/bulk Si	50	20	5	4000	60

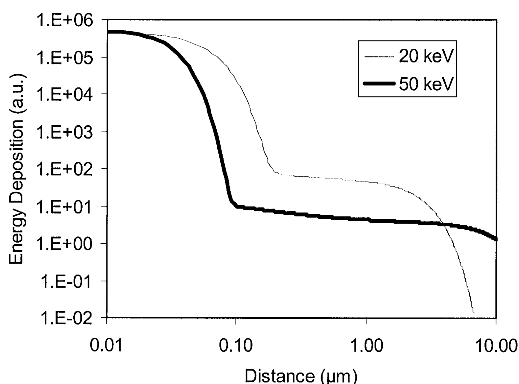

Fig. 3. EDF(r) due to "point" e-beam incident on 0.4 μm PMMA on bulk Si, for two widely used e-beam energies.

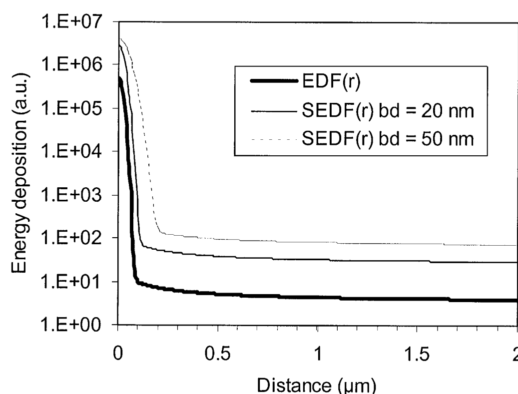

Fig. 4. Energy deposition spreading at the resist/substrate interface due to beam diameter (for a beam energy of 50 keV).

In Fig. 3 the EDF(r) for 20 keV and 50 keV e-beam energy in the case of 0.4 ìm on bulk Si is presented. This figure reveals a well-known phenomenon: the higher energy causes a more uniform backscattering contribution (larger area) while the contribution from the forward scattered electrons is localized closer to the Z-axis. Due to this behaviour the resolution is superior in the case of higher energies with the accompanied drawback of increased dose required.

The preference for higher e-beam energies is accompanied with the ability of e-beam lithography tools to deliver smaller beam diameters at higher e-beam energies. Even in that case the beam diameter has to be the smallest possible since it affects seriously the resist resolution. In Fig. 4 the SEDF(r) for various beam diameters is presented and compared with the EDF(r). The increase in beam diameter produces significant energy deposition in areas at longer lateral distances from the point of incidence. Since the total energy deposition does not depend on the beam characteristics but only on the exposure dose, it is obvious that at larger beam diameters the energy deposition at areas close to the point of incidence is smaller. In the next section the effect of beam diameter in final resist profile will be presented.

The EDF(r) and SEDF(r) are also valuable for proximity effect correction algorithms. The energy deposition is fitted with a sum of Gaussians. The coefficients and standard deviations of these

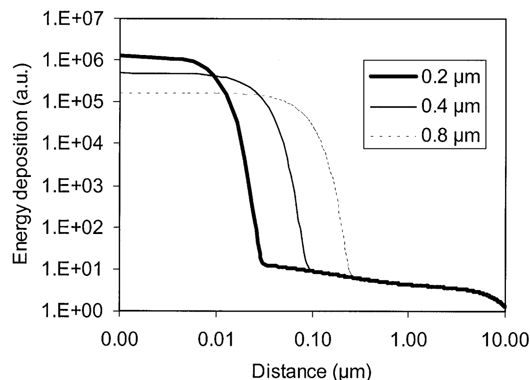

Fig. 5. EDF(r) at the resist/substrate interface for various resist thickness. The e-beam energy used was 50 keV.

Gaussians are used as input in the proximity effect correction software.

In Fig. 5 the effect of resist thickness on the energy deposition is presented. For thicker resist films the standard deviation of I_f (energy deposition due to forward scattered electrons) increases, therefore resolution decreases. Thus, from Figs. 3–5 it is obvious that, for the optimum resolution, the combination of thinner resist film — higher e-beam energy — best focus beam must be used.

As mentioned above, the use of multilayer substrates is common in electron beam lithography. In Fig. 2, EDF(r) for various substrates at the same resist thickness and e-beam energy is presented. The highest energy deposition takes place in the

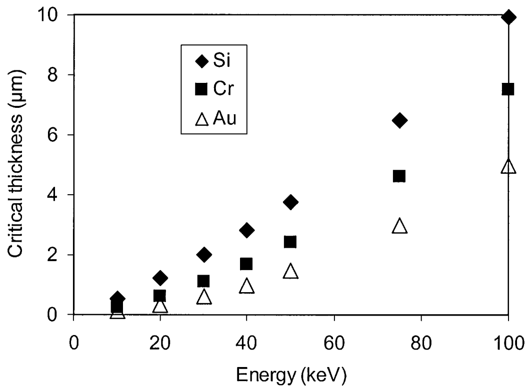

Fig. 6. T_{cr} as a function of e-beam energy for various materials (with different scattering parameters).

bulk Au substrate due to the higher scattering parameters this material has. Additionally, the energy deposition of backscattered electrons is more localized than in the other two cases (bulk Si, thin Au film over bulk Si), therefore the correction of proximity effect is more difficult and the resolution is limited. The multi-layer substrates will be used in the near future in a very important application: the fabrication of masks for EUV lithography where the mask plate consists of numerous thin layers of suitable reflective materials [12]. Therefore, the use of an accurate simulation tool will decrease the cost of mask fabrication significantly.

The extent of the intermediate layer effect depends on the material itself and the beam energy, whereas it is independent of the resist thickness. For every combination of beam energy and intermediate material (between resist and bulk substrate) there is a critical thickness T_{cr} beyond which the influence on the energy deposition is the same as that of a bulk substrate [7,13]. The dependence of T_{cr} on a wide range of e-beam energies for three different materials is presented in Fig. 6.

4. Resist development

The energy deposition is the most important quantity for electron beam lithography simulation in accordance with the importance of the aerial image in the simulation of optical lithography. The final energy deposition is used for the prediction of the resist profile under specific development conditions. The EDF(r) does not depend strongly on the resist material since almost all organic resists are polymers of C, H, O at different composition and of almost the same density. However, the development mechanism of each resist is different and generally it is difficult to develop a simple function that delineates the development mechanism and can be used for the prediction of the resist profile with great accuracy. For example, there are resists where the developer penetrates the resist film and causes swelling that decreases the resolution significantly, and other materials for which development time does not affect the resist profile. Therefore, for effective simulation a great effort must be applied to the development of such a function.

In the case of PMMA [14] a simple function has been developed [15] and used successfully for a long time. In this function the development rate depends on the local energy deposition and on some other parameters that can be measured by experimental techniques. In the current work, the parameter values needed for the development rate function have been calculated [16] using an experimental dissolution rate monitor (DRM) [17]. These values have been found to be different from those mentioned in the literature [16].

In Fig. 7a the effect of the beam diameter in the resist profile is presented by using the beam conditions mentioned in Fig. 4. It is obvious that the resist profile is completely different for the same exposure dose and development conditions. In the larger beam diameter case the linewidth is smaller than in the smaller beam diameter case. This effect is due to the wider spread of the same energy deposition in the large beam diameter case. Generally the large beam diameter decreases resist resolution significantly (Fig. 7b). This decrease is more intense at high beam energies (50–100 keV) where the standard deviation of forward scattering contribution (I_f) is small ($\sim$ 40 nm for 50 keV on 0.4 μm resist).

By using the development rate function mentioned above, extensive simulations have been carried out for the PMMA resist at different resist thicknesses. The layout consists of numerous very long lines with nominal linewidth (NLW) of 250

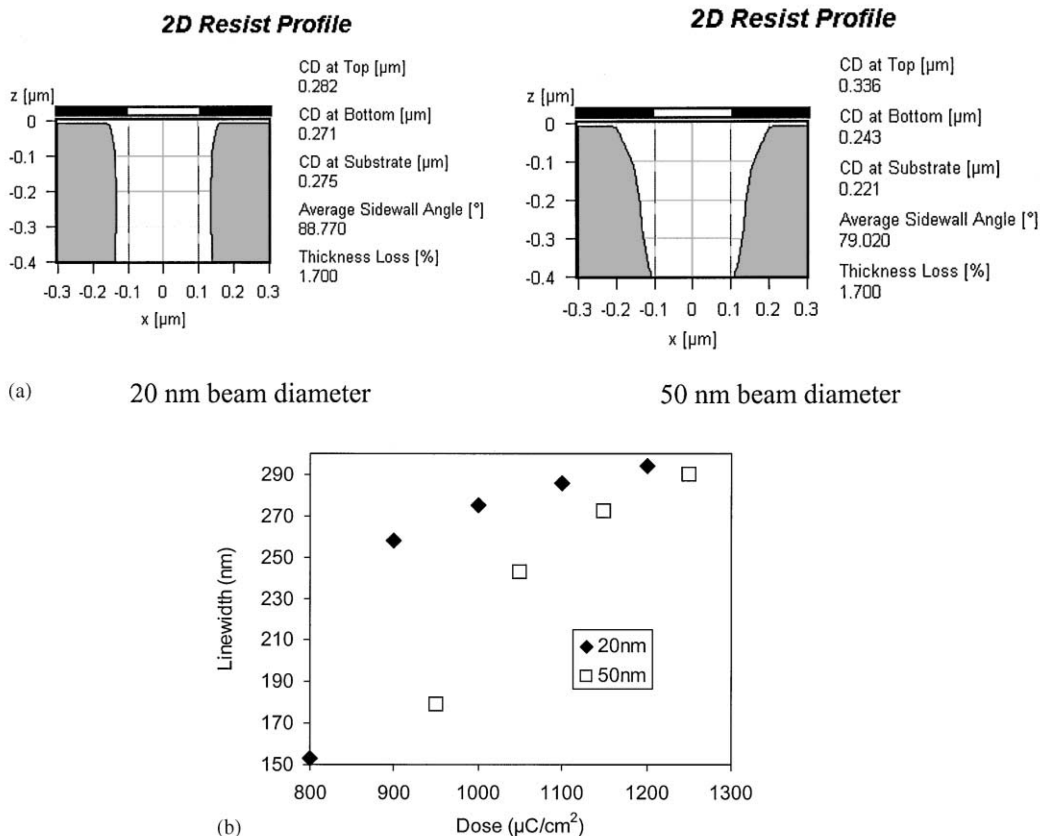

Fig. 7. (a) Resist profile of 0.2 μm isolated line (positive resist) produced at 50 keV beam energy with beam of 20 nm diameter (left) and of 50 nm (right) for the same exposure/development conditions. (b) linewidth vs. exposure dose for the two different beam diameters.

and 150 nm with spaces 500 and 300 nm, respectively. In Fig. 8 the simulation and experimental results are compared. The accuracy of simulation in all cases is satisfactory. The necessary exposures for the calculation of the development rate function and the high-resolution patterning were performed by a Leica EBPG-3 e-beam exposure tool operational at 20 and 50 keV. For the metrology a high-resolution SEM (LEO 440) was used.

In Fig. 9 the resist profiles (cross section) as predicted by the simulation and as revealed from the experiment are presented for two different exposure doses and two resist thickness. In Figs. 9a and b the resist thickness is 0.4 μm. In the lower dose the energy deposition was insufficient for total resist removal from the desired areas while at the higher dose the patterns revealed with larger than

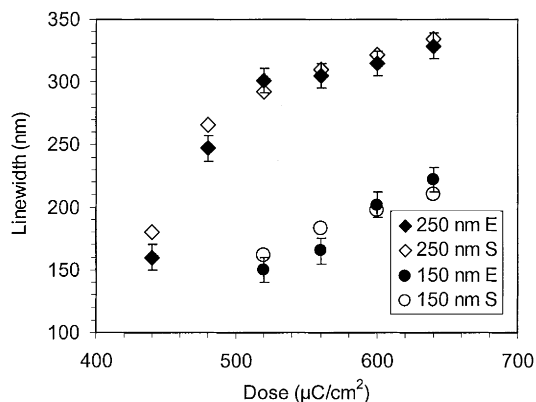

Fig. 8. Comparison of experimental (E) with simulation (S) results for 0.4 μm PMMA on bulk Si (50 keV). Pattern consists of 250 nm lines/500 nm spaces and 150 nm lines/300 nm spaces.

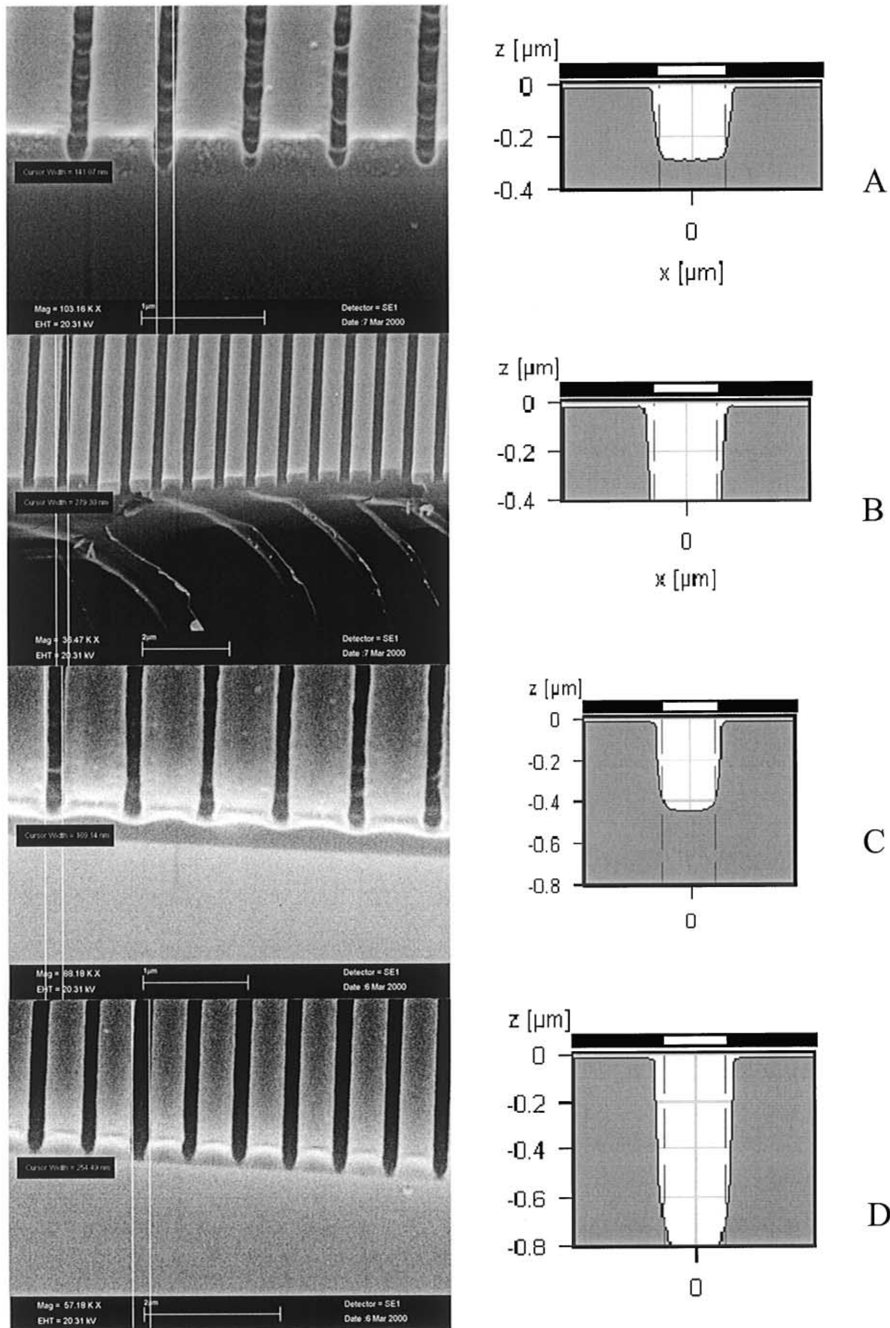

Fig. 9. Comparison of experimental (E) with simulation (S) results (pattern consists of 250 nm lines/500 nm spaces) for different exposures doses and resist thickness (A): 400 μC/cm^2, 0.40 μm PMMA, (B) 520 μC/cm^2, 0.4 μm PMMA (C) 440 μC/cm^2, 0.8 μm PMMA, (D) 560 μC/cm^2, 0.8 μm PMMA.

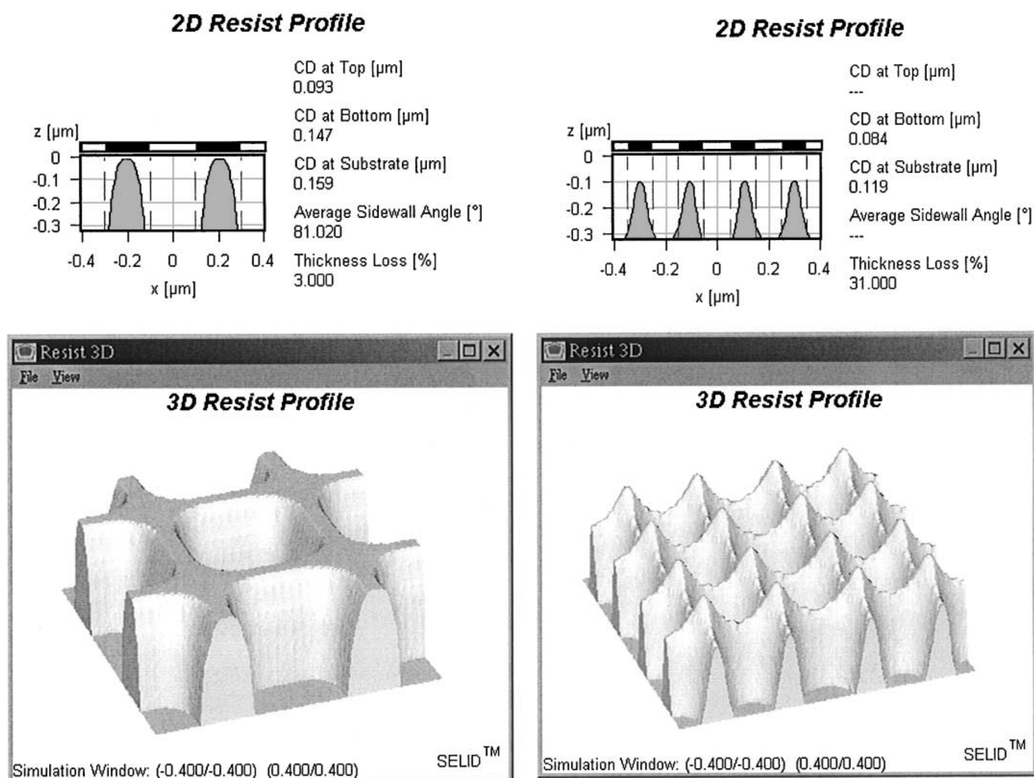

Fig. 10. Resist profiles (2-D and 3-D) of 200 nm dots/200 nm spaces (left) and 100 nm dots/100 nm spaces (right) on 0.32 μm initial resist thickness (PMMA) exposed at 50 keV. The significant thickness loss in unexposed regions in the 100 nm case is evident.

NLW dimensions. In Figs. 9c and d the resist thickness is 0.8 μm. Due to the development mechanism of PMMA a dose could be enough for complete removal of the resist in the desirable areas in thin layers (0.4 μm) while the same dose could be proved inadequate for thicker films (0.8 μm).

In parallel with the above comparisons, simulation has been carried out for another layout consisting of numerous holes (2-D matrix) of 200 and 100 nm NLW spaced by 200 and 100 nm, respectively. This type of layout is very useful for novel applications such as ultrahigh-density data storage devices, fluorescence study, development of catalysis nanocentres, etc. In Fig. 10, two- and three-dimensional simulation results are presented for both layouts. It is possible to pattern the 100 nm layout (using the specific experimental conditions: beam energy, pixel size, beam diameter). However the thickness loss is significant, an effect that makes difficult further processing (e.g. lift-off). Further improvement, could be obtained by using a smaller beam diameter and/or higher energy while the application of a thinner resist layer will introduce further problems in pattern transfer.

5. Conclusions

In the current work a fast electron beam lithography simulator (SELID™) has been used for the simulation of dense patterns in the 100–250 nm NLW range at high energies using the conventional positive-resist PMMA. Using that simulation tool the effects of beam diameter, beam energy and resist thickness have been studied in depth in order to extract the necessary values for high-resolution patterning. In order to improve the simulation's accuracy the development rate parameters have been

measured experimentally and found to be different from those published in the literature. The validity of these values has been verified from the simulation, where the use of literature values produces results far away from the ones observed experimentally.

Additionally, the simulator has been applied for a large area pattern consisting of 100, 200 nm dots spaced by 100, 200 nm for the development of a technology that can be used in the fabrication of novel devices.

Acknowledgements

The authors would like to thank TEI of Athens for the partial financial support of the work and Sigma-C for help in the simulations.

References

[1] DeJule R. Semicond Int 2000 2;23:66–76.
[2] Sato M, Ocola L, Novembre A, Ohmori K, Ishikawa K, Katsumata K, Nakayama T. J Vac Sci Technol 1999;B17:2873–7.
[3] Gordon M, Lieberman J, Petric P, Robinshon C, Stickel W. J Vac Sci Technol 1999;B17:2851–5.
[4] Rosenbusch A, Glezos N, Kalus M, Raptis I. Proc SPIE 1996;2884:435.
[5] Glezos N, Raptis I, Hatzakis M. Microelectron Engng 1994;23:417.
[6] Glezos N, Raptis I. IEEE Trans 1996; CAD 15: 92.
[7] Raptis I, Glezos N, Rosenbusch A, Patsis G, Argitis P. Microelectron Engng 1998;41/42:171.
[8] Paul BK. Microelectron Engng 1999;49:233–44.
[9] Cui Z. Microelectron Engng 1998;41/42:175–8.
[10] Cummings KD, Resnick DJ. J Vac Sci Technol 1988;B6:2033–6.
[11] Hasegawa S, Lida Y, Hidaka T. J Vac Sci Technol 1987;B5:142–5.
[12] Spector S, White D, Tennant D, Ocola L, Novembre A, Peabody M, Wood II,O. J Vac Sci Technol 1999;B17:3003–8.
[13] Raptis I, Meneghini G, Rosenbusch A, Glezos N, Palumbo R, Ardito M, Patsis G, Valamontes E, Argitis P. Proc SPIE 1998;3331:431.
[14] Hatzakis M. Appl Phys Lett 1971;18:7–9.
[15] Neureuther A, Kyser D, Ting C. IEEE Trans Electron Devices 1979;26:686–91.
[16] Velessiotis D, Raptis I. Unpublished results.
[17] Raptis I, Velessiotis D, Vasilopoulou M, Argitis P. Microelectron Engng 2000;53:489–92.